

Homopolymer Adsorption on Hexagonal Surfaces: A Replica-Exchange Monte Carlo Study

B Liewehr¹ and M Bachmann^{1,2,3}

¹Soft Matter Systems Research Group, Center for Simulational Physics,
The University of Georgia, Athens, Georgia, USA

²Instituto de Física, Universidade Federal de Mato Grosso, Cuiabá, Brazil

³Departamento de Física, Universidade Federal de Minas Gerais, Belo Horizonte, Brazil

E-mail: benjamin.liewehr@uga.edu, bachmann@smsyslab.org; <http://www.smsyslab.org>

Abstract. The adsorption behavior and thermodynamic properties of a coarse-grained flexible homopolymer, grafted on a hexagonal patterned surface, are investigated by means of parallel-tempering replica-exchange Monte Carlo simulations. In this study, the strength of the polymer-surface interaction, which is based on a standard Lennard-Jones potential, is changed systematically, mimicking different honeycomb-structured substrate materials. Utilizing specific order parameters, measured over a range of various temperatures and surface adsorption strengths, different structural phases are discriminated into classes of expanded, globular, droplet, and compact conformations. Finally, we construct the hyperphase diagram for a polymer with 55 monomers and discuss representative polymer structures.

1. Introduction

Recent research on two-dimensional nanomaterials revealed interesting surface properties, which are expected to lead to new applications in emerging technologies such as energy storage and novel electronic materials for integrated circuits. The most prominent example in this regard is graphene with outstanding mechanical, electrical, and thermal properties [1].

Since graphene as a semi-metal does not exhibit a band gap, which is required for many advanced applications like photovoltaics or field-effect transistors (FETs), structurally similar classes of materials have been investigated viz. transition metal dichalcogenides (TMX₂) and metal monochalcogenides (MX). Examples for these materials are MoS₂ or GaSe, exhibiting also hexagonal surface structures. These topological insulators and semiconductors allow for band gap engineering and thus show interesting optical properties such as photoluminescence. However, in contrast to pure graphene sheets, these materials are, in general, not chemically inert. Therefore, a protective coating is required to prevent reactions with the environment. Polymer coats are explored to serve this purpose [2, 3]. One key aspect of our study is the systematic investigation of polymer adsorption properties on generic hexagonal surfaces at different adsorption strengths, representing an entire class of miscellaneous substrates.

Graphene, as a potential substrate for drug delivery [1], may also be relevant for health care applications. Important in this context is the adhesion enhancement with polymers [4], as well as the compatibility with a biological environment [5, 6]. Therefore, it is necessary to understand the structural and thermodynamic behavior of such finite and comparatively small systems under thermal conditions. Since finite-size effects are essential for structure



formation on mesoscopic scales, qualitative changes of macrostate ensembles of such systems are not phase transitions in the conventional sense, because the thermodynamic limit is out of reach and scaling properties are typically not of interest. Key towards understanding these small interacting systems is the systematic investigation of the cooperative polymer adsorption behavior, which is currently only accessible by means of computer simulations. The system-inherent complexity generally entails a rugged free-energy landscape in the space of relevant degrees of freedom, requiring advanced generalized-ensemble Monte Carlo sampling methods [7]. In order to unravel the general adsorption behavior of polymer chains on surfaces, we employ a generic hybrid coarse-grained polymer-substrate model, in which the monomers in the linear polymer chain, representing entire chemical groups, are attracted by the interaction sites of the patterned substrate. The polymer is grafted with one end to the surface [8–10].

Here, we present first insights into the adsorption behavior of a flexible polymer at hexagonal surfaces for different adsorption strengths and temperatures. Dominant structural conformations are identified in this parameter space and enable the construction of a structural hyperphase diagram.

2. Polymer-substrate model and evaluation of the surface potential

In this adsorption study, the interactions of a homopolymer with $N = 55$ monomers are modeled by a potential U_{NB} describing the van-der-Waals polarization effects between non-bonded monomers of the polymer, by a bond potential U_{B} between subsequent polymer beads, and by the interaction U_{S} of each bead with the vertices of a hexagonally patterned substrate.

The non-bonded interaction is given by a shifted and truncated 12-6 Lennard-Jones (LJ) potential,

$$U_{\text{NB}}(r) = \begin{cases} U_{\text{LJ}}(r) - U_{\text{shift}}, & r < r_{\text{c}}, \\ 0, & \text{otherwise,} \end{cases} \quad (1)$$

with

$$U_{\text{LJ}}(r) = 4\epsilon \left[(\sigma/r)^{12} - (\sigma/r)^6 \right], \quad (2)$$

where r is the monomer-monomer distance and σ parametrizes the van-der-Waals radius of a monomer. The potential shift $U_{\text{shift}} = U_{\text{LJ}}(r_{\text{c}})$ is subtracted to avoid a discontinuity at the cutoff distance r_{c} . In our simulations, we fix the minimum location of the potential to $r_0 = 2^{1/6}\sigma \equiv 1$, the cutoff distance to $r_{\text{c}} = 2.5\sigma$, and set the energy scale ϵ to unity.

The bonded potential between adjacent monomers is based on the finitely extensible nonlinear elastic (FENE) potential [11–13]. A Lennard-Jones potential is added to account for the asymmetry of the bond due to volume exclusion and polarization,

$$U_{\text{B}}(r) = -\frac{1}{2}KR^2 \ln \left[1 - \left(\frac{r - r_0}{R} \right)^2 \right] + \eta(U_{\text{LJ}}(r) + 1) - 1 - U_{\text{shift}}. \quad (3)$$

The FENE potential restricts the bond extension to the interval $r \in [r_0 - R, r_0 + R]$, with parameters fixed to the typical values $R \equiv 3/7$ and $k \equiv 90/4$. The parameter η is set to $\eta \equiv 0.1$. The constant shift leads to the same minimum value for U_{B} as for U_{NB} .¹ One terminal monomer of the homopolymer chain is grafted to a vertex of the hexagonal surface. While the positions of the remaining $(N - 1)$ monomers are sampled, locations of surface sites are kept fixed in the $z = 0$ plane, allowing for a three-fold rotational symmetry and two linearly independent translational symmetries. The interaction between a monomer and a lattice site at the distance r is given by

$$U_{\text{S}}(r) = \epsilon_{\text{S}} U_{\text{NB}}(r), \quad (4)$$

¹ U_{B} can be shifted arbitrarily, because the number of bonds is kept constant. The shift leads only to an irrelevant overall energy constant.

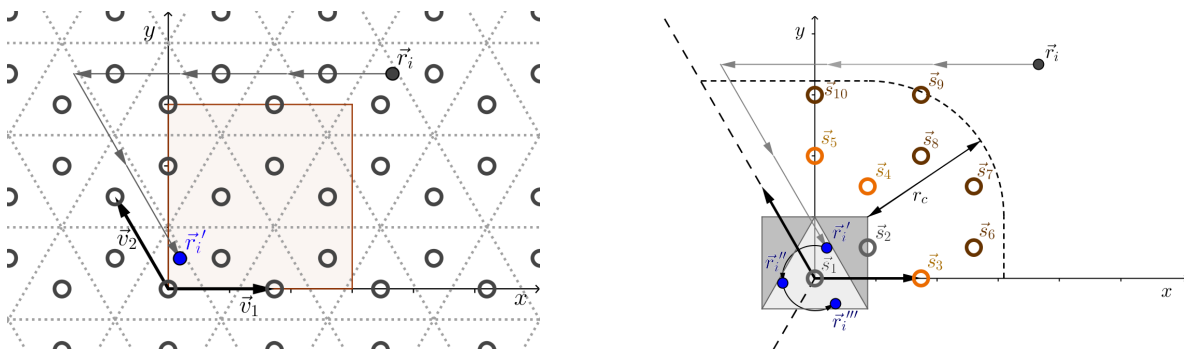


Figure 1. Hexagonal lattice structure of the substrate (circles). **Left:** Base vectors are denoted by $\vec{v}_1 = (\sqrt{3}, 0)^T$ and $\vec{v}_2 = (-\sqrt{3}/2, 3/2)^T$. The Wigner-Seitz cells are shown as dotted lines. If the monomer at position \vec{r}_i is translated into the basis cell, its new location is \vec{r}_i' ; rotation by $2\pi/3$ and by $4\pi/3$ yields \vec{r}_i'' and \vec{r}_i''' , respectively. **Right:** The gray rectangle marks the codomain of the lattice vector translation if applied to an arbitrary monomer position \vec{r}_i . The lattice sites located within the LJ-cutoff distance (dashed) are stored in sets of increasing distance to the codomain. The basis cell $\{\vec{s}_1, \vec{s}_2\}$ (gray) forms set 1, followed by set 2 $\{\vec{s}_3, \dots, \vec{s}_5\}$ (orange), and set 3 $\{\vec{s}_6, \dots, \vec{s}_{10}\}$ (brown).

where the parameter ϵ_S represents the surface adsorption strength. For simplicity, we choose the same cutoff radius r_c as for the non-bonded potential. In this study, the attraction strength of the surface was varied in the interval $\epsilon_S \in [0.0, 4.5]$, effectively representing different materials or solvent properties. The total energy of a conformation $\mathbf{X} = (\vec{r}_1, \dots, \vec{r}_N)$ with the monomer-monomer distance $r_{ij} = |\vec{r}_i - \vec{r}_j|$ and the distance $r_{ia} = |\vec{r}_i - \vec{s}_a|$ of a monomer i from a surface site a eventually reads,

$$E(\mathbf{X}) = \sum_{i=1}^{N-2} \sum_{j=i+2}^N U_{\text{NB}}(r_{ij}) + \sum_{i=1}^{N-1} U_{\text{B}}(r_{ii+1}) + \sum_{i=2}^N \sum_{a=1}^{\infty} U_{\text{S}}(r_{ia}). \quad (5)$$

For the evaluation of the last term in Eq. (5), it is computationally favorable to store the ten vertex positions $\vec{s}_1, \dots, \vec{s}_{10}$ of the basis cell, next-nearest cells, etc., in one $4\pi/3$ -sector (see Fig. 1) by utilizing the following algorithm.

First, a monomer \vec{r}_i is shifted by integer multiples of the lattice vectors towards the fundamental cell, where we assign to it the new position \vec{r}_i' . Second, two copies \vec{r}_i'' and \vec{r}_i''' are created by rotation about the z -axis by $2\pi/3$ and $4\pi/3$, respectively. The calculation of the distances r_{ia} between monomers and surface sites is performed in sets of $\{\{\vec{s}_1, \vec{s}_2\}, \{\vec{s}_3, \dots, \vec{s}_5\}, \{\vec{s}_6, \dots, \vec{s}_{10}\}\}$ (see Fig. 1, right), where the positions $\vec{s}_1, \dots, \vec{s}_{10}$ are sorted by increasing distance with respect to the origin of the coordinate system. The evaluation can be terminated as soon as all contributions from one set vanish. Finally, this procedure is applied to all monomers close to the surface, within LJ cutoff distance $z < r_c$.

In Fig. 2(top left), the effective potential $U_{\text{S}}(x, y, z)$ is plotted for $\epsilon_S = 1$ as a function of the lateral coordinates x, y in the distance $z = 0.81$ above the surface, probing the monomer positions in a triangular overlayer. This overlayer is observed for adsorbed compact phases, where monomers in the surface plane are located inside the centers of hexagons, i.e., on the vertices of the Wigner-Seitz cells depicted in Fig. 1(left). A small lateral translation of a polymer bead from this favored position results in a steep increase in energy compared to a vertical displacement (Fig. 2, top right). Vertical cuts of the surface potential along $y = 1$ and $x = \sqrt{3}$ at $z = 0.81$ are shown in Fig. 2(bottom left and right, respectively). Note that

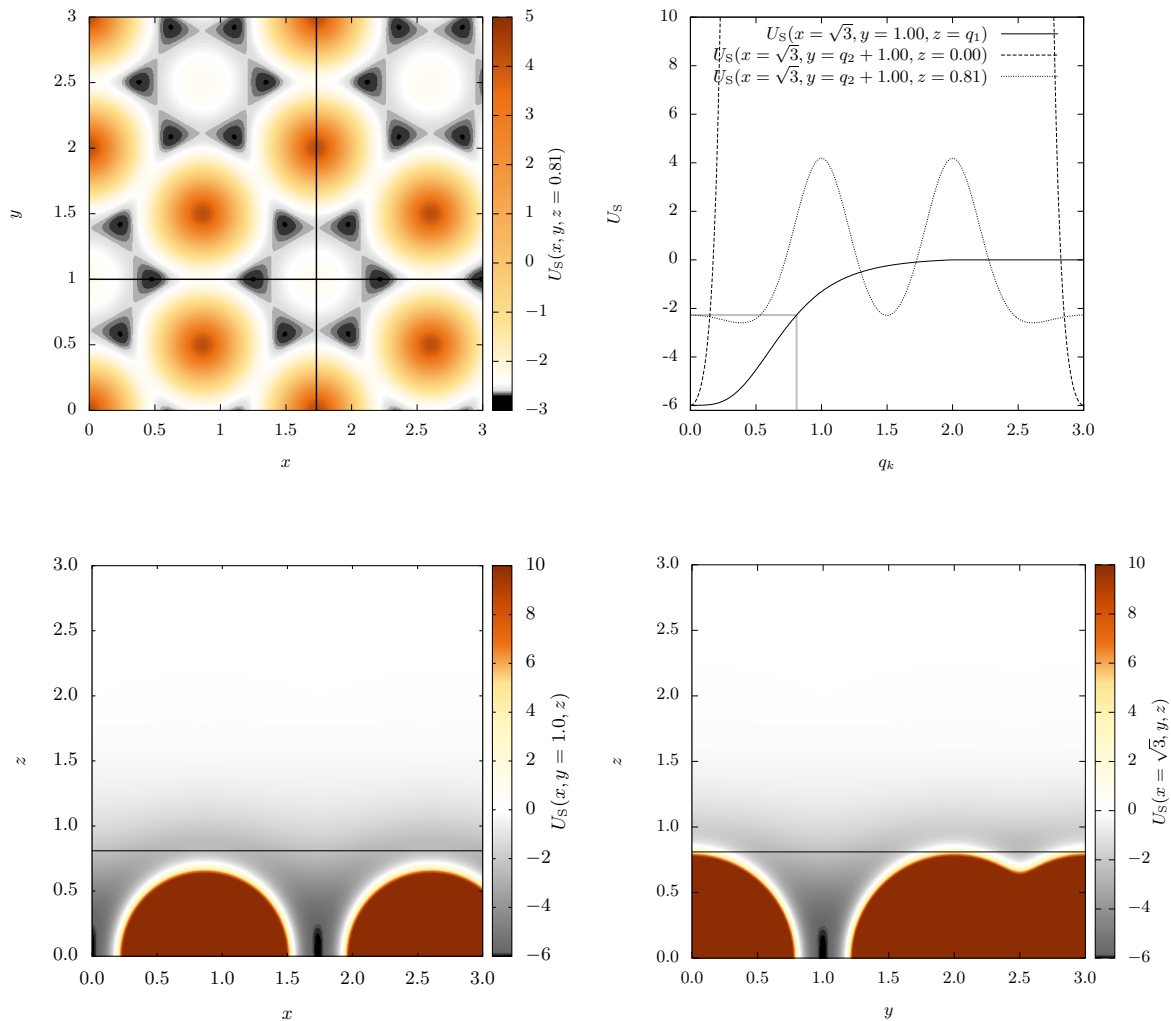


Figure 2. Representations of the surface potential $U_S(x, y, z)$ of the hexagonal substrate. **Top row:** (Left) Cut parallel to the surface at the height $z = 0.81$ of the triangular overlayer for the area marked in orange in the left-hand figure of Fig. 1. (Right) Potential as a function of favorable lattice site distance in perpendicular direction ($q_1 = z$, solid line), in a direction parallel to the surface ($q_2 = y - 1$), on the surface ($z = 0$, dashed), and above the surface ($z = 0.81$, dotted). **Bottom row:** Vertical cuts along $y = 1.0$ (left) and $x = \sqrt{3}$ (right). The height $z = 0.81$ is indicated by a horizontal line.

with increasing vertical distance the effective potential is smeared out. Thus, pattern effects are expected for polymer beads below $z = 1.5$ for this particular lattice type and parametrization of the potential.

3. Simulation method

The thermodynamic and structural properties of the 55-mer were investigated by means of data obtained in parallel tempering (replica exchange) Monte Carlo simulations at multiple temperatures, $T_1 < \dots < T_m < \dots < T_M$; $T_m \in [0.0, 5.0]$, uniformly distributed in inverse temperature space. Independent simulations were performed for a large number of surface attraction strengths $\epsilon_S \in [0.0, 4.5]$.

Whereas in each simulation the positions of surface sites were kept fixed, the conformational space of monomer positions was sampled at a given temperature T_m according to the Metropolis rule,

$$P_m(E_1 \rightarrow E_2) = \min(1, \exp[(E_1 - E_2)/k_B T_m]). \quad (6)$$

In every Monte Carlo sweep, a temperature-dependent displacement update was attempted for each non-grafted polymer bead. During the initial equilibration period, the maximum displacement was adjusted to allow for an acceptance rate of about 50%. Replica exchanges between temperature threads facilitated melting and freezing, i.e., decorrelation of polymer conformations. An exchange between neighboring temperature threads (T_m, T_k) was proposed after every 10^3 Monte Carlo sweeps and accepted with the exchange probability,

$$P_{mk}(E_m, T_m \leftrightarrow E_k, T_k) = \min(1, \exp[(E_m - E_k)(1/k_B T_m - 1/k_B T_k)]) \quad (7)$$

As the initial configuration in each thread we used the lowest-energy state found in a short test run. After thermodynamic equilibrium was reached, each simulation with fixed ϵ_S value comprised 10^5 replica exchange attempts per thread.

Thermodynamic properties were investigated by analyzing the canonical mean values such as energy $\langle E \rangle(T)$, components of the radius of gyration parallel and perpendicular to the surface, $\langle r_{\text{gyr},\parallel} \rangle(T)$ and $\langle r_{\text{gyr},\perp} \rangle(T)$, respectively, the end-to-end distance $\langle l_{\text{ee}} \rangle(T)$, and number of contacts $\langle n_s \rangle(T)$ at thread temperatures T_m .

Transition temperatures were identified by means of peaks and “shoulders” in fluctuation curves of a quantity O , given by

$$\frac{d}{dT} \langle O \rangle = \frac{\langle OE \rangle - \langle O \rangle \langle E \rangle}{k_B T^2}. \quad (8)$$

For example, the heat capacity $C_V = d\langle E \rangle/dT$ accounts for energetic fluctuations. Multiple-histogram reweighting [14] was employed to calculate the density of states $g(E)$ from individual estimates obtained in each temperature thread. The resolution of energy histograms was chosen as $dE = 0.05$. With the density of states at hand, energetic quantities and fluctuations were calculated as continuous functions of temperature, which enabled us to locate transition signals between the simulation temperatures T_m more precisely.

Since the system is of finite size, transition signals identified in different response quantities for the same specific structural transition do not typically coincide. Therefore, this information was accumulated in T - ϵ_S parameter space in transition bands rather than transition lines. Phases separated by these bands were characterized by means of the polymer geometry, initially by analyzing similarity features of $10^2 - 10^3$ conformations within a single phase. This geometric characterization allowed for the introduction of phase-specific order parameters, which are described in the following section.

4. Adsorption on a hexagonal surface

4.1. Structural hyperphase diagram

A schematic overview of the adsorption behavior of the flexible homopolymer is presented in the T - ϵ_S hyperphase diagram shown in Fig. 3. As mentioned earlier, transition signals from different quantities are observed within a broad transition band, rather than at a unique transition temperature. Transition bands in Fig. 3 are indicated by gray lines, separating different structural phases which are annotated by a letter code, similar to the labels introduced in Ref. [9].

At high temperatures $T > 1.5$ and small adsorption strengths, the polymer resides primarily in the phase of desorbed expanded conformations (DE), which is well known from unconstrained

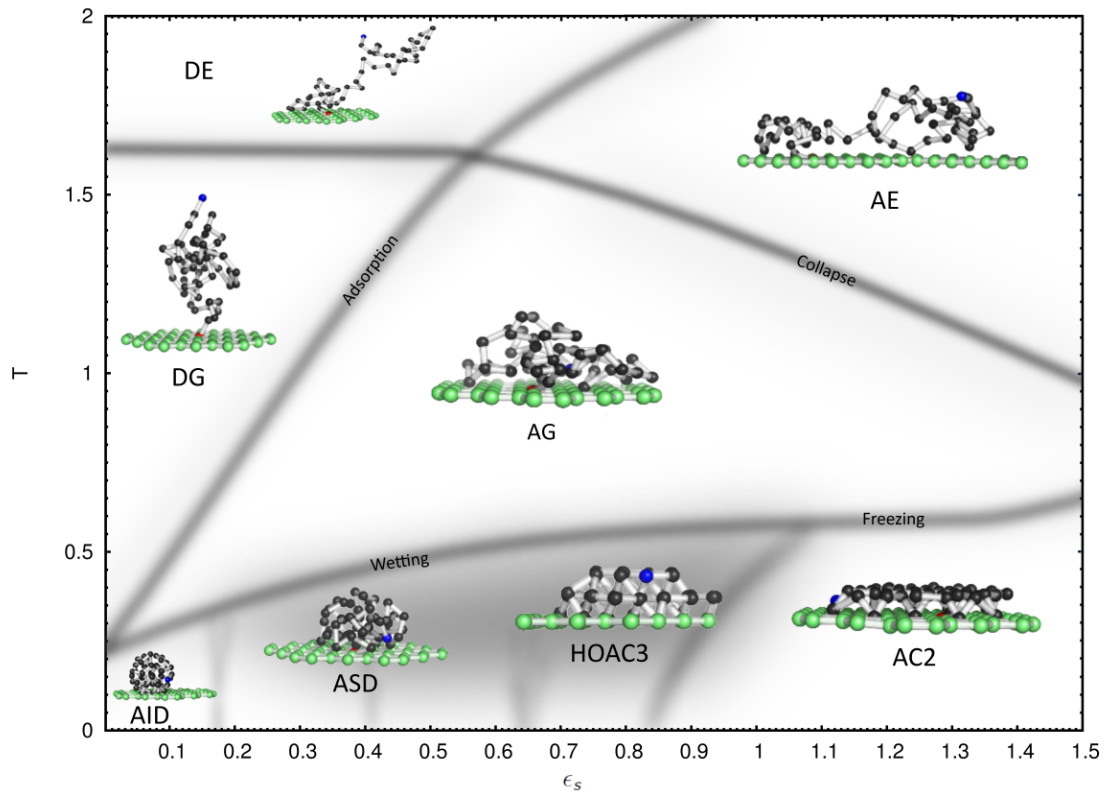


Figure 3. The structural T - ϵ_s hyperphase diagram is shown with typical conformations superimposed. At high temperatures and small adsorption strengths, the desorbed expanded (DE) conformations dominate. By crossing the adsorption transition line, the DE phase goes over into the adsorbed expanded (AE) phase for higher surface adsorption strength ϵ_s . Below the collapse transition band, adsorbed and desorbed globular phases are found. At low temperatures and depending on the surface attraction strength, adsorbed icosahedral droplets (AID) or semispherical droplets (ASD) form. For adhesion strengths $\epsilon_s > 0.8$, highly oriented adsorbed compact structures arranged in 3 layers (HOAC3) and adsorbed compact conformations (AC2) prevail.

homopolymers. For increased surface adsorption strength ϵ_s , these structures are found closer to the surface, within the Lennard-Jones cutoff $z < r_c$. Conformations in this regime are in energetic contact with the surface, but the pattern of the substrate is not yet recognized by the polymer. This polymer behavior defines the adsorbed expanded phase (AE). It is observed that the polymer beads in this phase are primarily located at rather large distances $1.5 < z < r_c$ where the surface potential is smeared out [see Fig. 2(top right)]. Therefore, the structural features in this phase compare well to the adsorption on continuous surfaces [15].

At low temperatures, generally compact polymer conformations govern the solid phases. Typical for a flexible homopolymer with 55 constituents is a crystalline structure with icosahedral shape. An icosahedron is characterized by 20 equally shaped tetrahedra. We find it attached to the surface in phase AID (adsorbed icosahedral droplet) if the surface adsorption strength approaches zero. The shortest polymer chain forming such a structure is the 13-mer. Therefore, the 55-mer possesses an icosahedral core of 13 monomers while the remaining 42 monomers form the complete overlayer.

The more interesting and model parameter specific features are found for $\epsilon_s > 0$. Already for

small surface interactions the symmetry of the icosahedral ground state is broken and adsorbed semi-spherical droplet-like (ASD) conformations dominate. At adsorption strengths $\epsilon_s > 0.8$ patterned structures are found. The number of surface contacts is a suitable order parameter that allows to distinguish the ordered phases, in which the surface pattern is recognized by the polymer, from disordered phases. It is defined as the number of monomers below a certain threshold distance z_{lim} to the surface and its fluctuation behavior is particularly useful for the identification of transition lines between these phases. One of the most interesting patterned subphases is HOAC3, which is dominated by highly oriented adsorbed compact 3-layer structures (see Fig. 3).

4.2. Thermodynamic and structural order parameters

One of the key challenges in this study is that surface-specific phases are found at very low temperatures, where parallel tempering generally suffers from large correlations that cause an effective slowing-down of the simulation. Moreover, structures in these phases depend sensitively on values of the surface adsorption strength ϵ_s . Consequently, we expect more subphases at low temperatures in the regime of droplet-like and patterned conformations [16]. Since signals in this regime are much weaker than for more prominent transitions, i.e., the freezing transition or coil-globule transitions, we suppose that subphases in the regime of droplet conformations are separated by steep (vertical) transition bands. In Fig. 3, these transitions are sketched in the interval $\epsilon_s \in [0.1, 1.1]$. With parallel tempering, they can only be identified if the ϵ_s -parameter space is scanned with high resolution and high accuracy of suitable order parameters. A useful parameter that describes the effective distance of the homopolymer from the surface is the z -component of the center of mass. In a similar way, fluctuations about the mean of the sum over all surface interactions, which is the last term in Eq. (5), signal these transitions as well.

More specific is the average number of surface contacts, i.e., the number of monomers located near the surface below z_{lim} . In particular in the phase HOAC3 (cf. Fig. 3), the monomers that are arranged in three layers are well separated by the threshold values $z_{\text{lim}} \in \{0.3, 1.0, 1.5\}$. The latter value, for instance, is used to signal the freezing transition from the adsorbed globule (AG) into the highly oriented adsorbed compact (HOAC3) phase, since the number of surface contacts $n_{s,1.5}$ discriminates monomers that reside above the ordered layers which do not belong to the crystalline conformation.

In addition, we consider the threshold for an energetic contact with the surface given by the LJ cutoff $r_c \approx 2.23$. For small surface adsorption strengths, the fluctuation signals of $n_{s,0.3}$ compare well with the peaks in the heat capacity C_V . Furthermore, fluctuations of $n_{s,1.0}$ suggest vertical separations of droplet and globular subphases. For increasing surface adsorption strengths, polymer conformations become flatter (wetting). The divergence of the FENE potential at maximum bond length prevents the occupation of favorable lattice sites by two adjacent monomers of the homopolymer. Thus, at least one additional monomer is required to link monomers residing in the centers of neighboring hexagons. In the simplest case, three monomers form a *zig-zag* bridge, with the central monomer located above the surface. However, the repulsive character of the surface potential near the interaction sites of the substrate, as it is felt by the central monomer (Fig. 2, bottom row), requires that either monomers in the surface layer slightly lift off from the hexagonal plane or that bonds are stretched. Therefore, the formation of *zig-zag* bridges is strongly dependent on the surface adsorption strength. In the AC2 phase, *zig-zag* bridges can occur at the edge of the film-like structure.

Towards the center of typical AC2 conformations (“bulk”), beads in the second layer ($z \approx 0.81$) form a regular triangular lattice. The bond length of bonded monomers located in two different layers typically corresponds to the equilibrium distance r_0 . Obviously, the formation of the triangular overlayer requires more beads than are necessary to fill favorable lattice sites in the underlying surface layer. In this phase, we observe a ratio $(\langle n_{s,1.0} \rangle - \langle n_{s,0.3} \rangle) / \langle n_{s,0.3} \rangle \approx 3$. For

higher surface adsorption strengths, $\epsilon_S > 2$, the formation of a triangular overlayer is reduced in favor of *zig-zag* bridges, leading to a larger number of surface contacts $n_{s,0.3}$.

5. Conclusion

In this work, we have studied the cooperative adsorption behavior of a generic polymer model interacting with a hexagonally patterned substrate by means of parallel-tempering replica-exchange Monte Carlo simulations. The interaction strength between the homopolymer and the surface was varied systematically.

To locate structural phase transition bands, we extracted canonical and structural quantities from sampled configurations and applied canonical statistical analysis. Different structural phases were characterized, allowing for the identification of pattern recognition effects by the homopolymer. We summarized these results by constructing a complete hyperphase diagram, parametrized by the temperature T and the surface adsorption strength ϵ_S . Depending on the adsorption strength, we found for low temperatures $T < 0.5$ specific wetting and freezing transitions into phases dominated by adsorbed droplet-like and crystal-like conformations. For high temperatures, $T > 1$, the entropic enhancement prevents pattern recognition by the polymer. In the phases of globular and extended structures, most monomers reside in a distance from the surface where patterns in the potential are averaged out.

The hyperphase diagram of adsorption for a flexible polymer near a hexagonal substrate exhibits a large number of characteristic and unique features. Depending on the surface adsorption strength and temperature, we identified different adsorption scenarios for surface wetting/dewetting and pattern recognition. Prospectively, this allows for both, the classification of surfaces with respect to polymer adsorption and it helps understand how different polymers adsorb on a certain substrate of interest. These questions are apparently of interest for the design of hybrid materials composed of soft and solid matter.

Acknowledgments

B. Liewehr acknowledges support by the *Studienstiftung des deutschen Volkes* and through the exchange program between the University of Rostock and the University of Georgia. This work has been supported partially by the NSF under Grant No. DMR-1207437 and by CNPq (National Council for Scientific and Technological Development, Brazil) under Grant No. 402091/2012-4.

References

- [1] Novoselov K S, Fal'ko V I, Colombo L, Gellert P R, Schwab M G and Kim K 2012 *Nature* **490** 192–200
- [2] Potts J R, Dreyer D R, Bielawski C W and Ruoff R S 2011 *Polymer* **52** 5–25
- [3] Alexandre M and Dubois P 2000 *Materials Science and Engineering: R: Reports* **28** 1–63
- [4] Sides S W, Grest G S and Stevens M J 2001 *Physical Review E* **64** 050802
- [5] Wei Q, Becherer T, Angioletti-Uberti S, Dzubiella J, Wischke C, Neffe A T, Lendlein A, Ballauff M and Haag R 2014 *Angewandte Chemie International Edition* **53** 8004–8031
- [6] Carignano M and Szleifer I 2000 *Colloids and Surfaces B: Biointerfaces* **18** 169–182
- [7] Bachmann M 2014 *Thermodynamics and Statistical Mechanics of Macromolecular Systems* (Cambridge University Press, Cambridge)
- [8] Li T and Park K 2001 *Computational and Theoretical Polymer Science* **11** 133–142
- [9] Möddel M, Janke W and Bachmann M 2011 *Macromolecules* **44** 9013–9019
- [10] Möddel M, Janke W and Bachmann M 2014 *Physical Review Letters* **112** 148303
- [11] Bird R B, Curtiss C F, Armstrong R C and Hassager O 1987 *Dynamics of Polymeric Liquids* 2nd ed (Wiley, New York)
- [12] Kremer K and Grest G S 1990 *Journal of Chemical Physics* **92** 5057–5086
- [13] Milchev A, Bhattacharaya A and Binder K 2001 *Macromolecules* **34** 1881–1893
- [14] Ferrenberg A M and Swendsen R H 1989 *Physical Review Letters* **63** 1195–1198
- [15] Pattanasiri B, Liewehr B and Bachmann M 2015 *Physics Procedia* **68** 90–94
- [16] Liewehr B and Bachmann M 2015 *to be published*